ISSN 0304-9892 (Print) ISSN 2455-7463 (Online)
www.vijnanaparishadofindia.org/jnanabha

Jñānābha, Vol. 55(2) (2025), 278-296

MODELING THE IMPACT OF ANTHROPOGENIC TEMPERATURE RISE ON THE DYNAMICS OF CARRIER-DEPENDENT INFECTIOUS DISEASES

Ranjeet Kumar[1] and S. N. Mishra[2,*]
[1,2]Department of Mathematics, B.N.D. College, C.S.J.M. University, Kanpur, Uttar Pradesh, India-208004
Email: 1507dr@gmail.com, *s.n.mishra_kn05@csjmu.ac.in (Corresponding author)
(Received: November 13*, 2025; In format: November* 16*, 2025; Revised: December* 27*, 2025; Accepted: December* 30*, 2025)*

DOI: https://doi.org/10.58250/jnanabha.2025.55230

Abstract

Anthropogenic activities are the primary drivers of the rising global average temperature, profoundly affecting carrier population and thereby intensifying the spread and dynamics of carrier-dependent infectious diseases. In this study, we develop a non-linear mathematical model to investigate the impact of temperature rise on disease transmission. The model incorporates four key dynamical variables: global temperature (elevated due to human-induced factors), the densities of susceptible and infected human populations, and the density of the carrier population. The carrier population is assumed to grow logistically, with its intrinsic growth rate influenced by rising temperature and its carrying capacity affected by human activities. The model is analyzed using the stability theory of differential equations and supported by numerical simulations based on biologically relevant parameter values. The results indicate that increasing global temperature accelerates carrier population growth, which, in turn, contributes to a rise in the number of infections within the human population.
2020 Mathematical Sciences Classification: 34C60, 92D40, 37N25, 92D30, 37N30.
Keywords and Phrases: Mathematical model, Carrier population, Anthropogenic activities, Global average temperature, Numerical simulation.

1 Introduction

Climate change is one of the biggest problems facing the world today. One major result of climate change is the continuous rise in global temperature, mainly caused by human activities such as burning fossil fuels, cutting down forests, running industries, and using chemicals in farming. These actions release greenhouse gases into the air, which trap heat and make the Earth warmer over time. This rise in temperature affects many parts of life, including human health and the spread of diseases [8, 11]. These diseases that spread through contaminated food, are often with the help of carriers like houseflies. Houseflies do not cause diseases themselves, but they carry germs from dirty places like garbage, drains, or open toilets, and spread them to uncovered or poorly handled food. This can lead to illnesses such as typhoid and diarrhea, especially in areas with poor hygiene and sanitation [24, 26]. As temperature increases, houseflies grow and reproduce more quickly. Warm conditions allow them to survive longer, lay more eggs, and become more active. This leads to a rise in their population, which increases the chances of disease-causing germs being spread to food. In addition, high temperatures can also help germs survive and multiply faster in food and the surrounding environment [12, 13]. The 21^{st} century has witnessed a sharp acceleration in global environmental transformations, largely attributed to intensified anthropogenic activities. Among these transformations, global warming characterized by a persistent increase in the Earth's average surface temperature has emerged as one of the most pressing environmental and public health concerns worldwide. One significant consequence of this warming is the increased carrier population and the corresponding rise in the spread of food-borne diseases [35, 36].

Food-borne illnesses represent a critical and persistent global public health challenge, contributing substantially to both morbidity and mortality across populations worldwide. These diseases exert their most devastating effects in low and middle income countries, where inadequate sanitation, limited access to clean water, poor food-handling practices, and insufficient health infrastructure amplify the risk of infection. According to the World Health Organization (WHO) [37, 38, 39], it is estimated that nearly 600 million

individuals, almost one in ten people globally fall ill each year due to the consumption of contaminated food, leading to approximately 420,000 deaths annually. This staggering burden highlights the profound impact of food-borne diseases on public health, economic stability, and overall quality of life. Among the wide range of illnesses transmitted through contaminated food, notable examples include typhoid fever, dysentery, shigellosis, cholera, and various forms of bacterial and viral gastroenteritis. These diseases are often associated with pathogens that proliferate under unsanitary environmental conditions, finding ideal transmission routes through food and water sources. One of the most significant yet often underestimated vectors in this transmission chain is the common housefly (Musca domestica), which plays a crucial role as a mechanical carrier of infectious agents. Due to their natural feeding and breeding behaviors, houseflies frequently come into contact with fecal matter, garbage, decaying organic substances, and other reservoirs rich in microbial contaminants. After acquiring pathogens from these sources, flies can easily transfer them to human environments. When they subsequently alight on exposed food, kitchen utensils, food preparation surfaces, or open wounds, they facilitate the transmission of numerous disease-causing microorganisms. This process occurs through physical contact, regurgitation, or excretion, all of which can contaminate human food supplies. Numerous studies have confirmed that houseflies are capable of harboring and disseminating an extensive range of pathogenic organisms-including bacteria such as Salmonella spp., Escherichia coli, and Shigella spp., as well as a variety of viruses, fungi, and protozoan cysts [1, 2, 3]. In fact, it has been reported that a single fly can carry more than one hundred distinct pathogenic species, underlining their epidemiological significance in the context of food-borne disease transmission. The ubiquity of houseflies in both urban and rural environments, coupled with their rapid breeding cycles and close association with human habitats, makes them a persistent threat to food safety and public health. Consequently, understanding their ecological behavior, transmission dynamics, and the environmental factors that influence their population growth is essential for developing effective strategies to mitigate the spread of food-borne diseases [4, 5, 6].

During the past few decades, numerous mathematical models [27, 28, 29] have been developed to capture the dynamics of the proliferation of infectious diseases. These models serve as essential tools for understanding disease transmission, assessing risk factors, predicting outbreak patterns, and evaluating the effectiveness of various intervention strategies. The role of carrier populations in disease transmission has also been extensively examined through mathematical modeling frameworks. Notably, Singh *et al.* [30, 31] formulated a model in which the carrier population was assumed to follow logistic growth dynamics, with both the intrinsic growth rate and carrying capacity modeled as functions of the human population density. This approach provides valuable insight into how human-driven environmental changes influence carrier proliferation and, consequently, the spread of infectious diseases. Naresh *et al.* [23] proposed and analyzed a nonlinear vaccination model to study the spread of carrier-dependent infectious diseases under the influence of environmental factors. Their analysis demonstrated that if the vaccination rate exceeds a critical threshold, the disease cannot escalate into an epidemic provided that the carrier population remains at its equilibrium level. This result underscores the dual importance of both vaccination efforts and effective management of the carrier population in disease control. Misra *et al.* [20, 21] developed a mathematical model showing that using chemical insecticides based on the number of carriers can help reduce the density of the carrier population. They found that spraying insecticides on time is effective, but delays in spraying may destabilize the system and increase the risk of disease. A recent study by, Singh *et al.* [33, 34] proposed a nonlinear mathematical model to analyze the effect of temperature on the transmission of carrier-dependent infectious diseases. The model incorporates temperature as a dynamic variable influencing the intrinsic growth rate and carrying capacity of the carrier population. Through stability analysis and numerical simulations, the study demonstrated that rising temperature especially those driven by anthropogenic activities can lead to a significant increase in the carrier population and, consequently, the number of infected individuals.

This research aims to explore the intricate relationship between carrier populations and global temperature, which is elevated due to anthropogenic activities, with particular emphasis on contamination pathways. The carrier population is assumed to grow logistically, with its intrinsic growth rate influenced by rising temperatures and its carrying capacity affected by human activities. By investigating these interactions, the study seeks to enhance our understanding of the transmission dynamics of food-borne diseases in the context of a warming climate. Such insights are essential for identifying effective strategies to control carrier populations and mitigate the public health risks associated with food-borne infections.

2 Mathematical model

For the model formulation, suppose the total human population in the considered region at the time t be denoted by $N(t)$, which is divided into two classes, namely susceptible population $X(t)$ and the infected population $Y(t)$. The density of carrier population in the considered region is represented by $C(t)$, while the global average temperature represented by $T(t)$, elevated due to anthropogenic activities. The susceptible population is assumed to grow at a constant rate A, which comprehends both birth and immigration to the considered region. The disease is assumed to spread both through direct contact between susceptible and infected individuals at a rate βXY, and indirectly through carriers that contaminate food consumed by susceptible individuals [14, 15]. As food-borne diseases spread via carriers, therefore we have considered that the susceptible population moves to infected population at a rate $\lambda XC/(m+C)$, where λ represents the disease transmission rate and m is the half saturation constant. Recovered individuals do not develop permanent immunity and can be reinfected; thus, the parameter ν denotes the recovery rate. The parameters α and d are introduced to represent the disease-induced and natural death rates of the human population, respectively. The carrier population is assumed to follow logistic growth, characterized by an intrinsic growth rate $r_0$and a carrying capacity k_0. However, temperature significantly influences the intrinsic growth rate of the carrier population. Elevated temperatures accelerate the carriers reproduction and developmental processes and extend their breeding season, resulting in an increase in their population [16, 17]. Therefore, the intrinsic growth rate is considered as a temperature-dependent function $r(T)$, while the carrying capacity is assumed to increase with the human population and is represented as $k(N)$. Further, carrier population depletes due to various unfavorable environmental factors, which is incorporated by the term r_2C. Hence, our proposed model system reads as follows:

$$\begin{aligned}
\frac{dT}{dt} &= pN - \alpha_0(T - T_0),\\
\frac{dX}{dt} &= A - \beta XY - \lambda X\frac{C}{m+C} - dX + \nu Y,\\
\frac{dY}{dt} &= \beta XY + \lambda X\frac{C}{m+C} - (\nu + \alpha + d)Y,\\
\frac{dC}{dt} &= r(T)C - r_0\frac{C^2}{k(N)} - r_2C.
\end{aligned} \tag{2.1}$$

We define the temperature-dependent intrinsic growth rate and the population-dependent carrying capacity of the carrier population as $r(T) = r_0 + r_1T$, $k(N) = k_0 + k_1N$ respectively. Here, r_1 and k_1 represent the incremental coefficients corresponding to the effects of temperature on the intrinsic growth rate and of human population on the carrying capacity. The initial conditions for the system are given by $T(0) = T_0 > 0$, $X(0) = X_0 > 0, Y(0) = Y_0 \geq 0$, and $C(0) = C_0 \geq 0$. The constant T_0 denotes the global average temperature of the pre-industrial era, which serves as the baseline reference level for temperature variation in the model. The various parameters used in the model are described in Table 6.1. We take into consideration the following reduced system (using $X + Y = N$) in order to analyze model (2)

$$\begin{aligned}
\frac{dT}{dt} &= pN - \alpha_0(T - T_0),\\
\frac{dY}{dt} &= \beta(N - Y)Y + \lambda\frac{C(N-Y)}{m+C} - (\nu + \alpha + d)Y,\\
\frac{dN}{dt} &= A - dN - \alpha Y,\\
\frac{dC}{dt} &= r(T)C - r_0\frac{C^2}{k(N)} - r_2C.
\end{aligned} \tag{2.2}$$

Lemma 2.1. *Following set defines the region of attraction for model system* (2.2)*:*

$$\Omega = \{(T, Y, N, C) \in \mathbb{R}^4_+ : T_0 \leq T \leq T_m, 0 \leq Y \leq N \leq \frac{A}{d}, 0 \leq C \leq C_m\},$$

where $T_m = T_0 + \dfrac{pA}{\alpha_0 d}$ *and* $C_m = \left\{\dfrac{r(T_m)k(A/d) - r_2}{r_0}\right\}$ *and it attracts all the solutions that initiate in the interior of the positive orthant.*

3 Basic reproduction number (R_0)

The disease-free equilibrium point, denoted by E_0, is obtained by setting $C = 0$ and $Y = 0$. Under this condition, the infectious components of the model system (2.2), can be expressed as follows:

$$\begin{aligned}\frac{dY}{dt} &= \beta(N-Y)Y + \lambda\frac{C(N-Y)}{m+C} - (\nu+\alpha+d)Y,\\ \frac{dC}{dt} &= r(T)C - r_0\frac{C^2}{k(N)} - r_2C.\end{aligned} \tag{3.1}$$

The corresponding matrix is:

$$P = \begin{bmatrix}\beta(N-Y)Y + \lambda\frac{C(N-Y)}{m+C}\\ 0\end{bmatrix},$$

$$S = \begin{bmatrix}(\nu+\alpha+d)Y\\ \left(-r(T) + r_0\frac{C}{k(N)} + r_2\right)C\end{bmatrix}.$$

The basic reproduction rate R_0 is given by

$$R_0 = \text{(individual infection rate) (individual recovery rate) }^{-1}.$$

This concept is extended to matrices in the next generation approach. The next generation matrix divides the compromised system into two matrices of rates when there are several infection kinds to monitor. These rate matrices are typically referred to as F and V:

$$\begin{aligned}M &= [infection\ rates] \times [recovery\ rates]^{-1}\\ &= F \times V^{-1}.\end{aligned}$$

As a result, the transition matrices (F and V) related to the equilibrium state E_0 are derived as follows.

$$F = \begin{bmatrix}\frac{\beta A}{d} & \frac{\lambda A}{dm}\\ 0 & 0\end{bmatrix},$$

and

$$V = \begin{bmatrix}(\nu+\alpha+d) & 0\\ 0 & (-r(T_m)+r_2)\end{bmatrix}.$$

In the model system (2.2), the basic reproduction number (R_0) is the spectral radius (largest eigenvalue) of the next generation matrix (N.G.M): $R_0 = \rho(FV^{-1})$ [18, 19]. Therefore, we obtain

$$R_0 = \frac{\beta A}{(\nu+\alpha+d)d}.$$

4 Equilibria of the proposed system

The model system (2.2) is nonlinear; therefore, it is not possible to find its exact solution. Utilizing the stability theory of differential equations, we therefore investigate the system's long-term behavior, identify the model's equilibrium, and look at the stability analysis of the equilibria. An equilibrium point that does not change with time of a dynamical system is the solution [7, 9]. These points are obtained by putting the growth rate of different variables of the model system equal to zero. The model system (2.2) manifests three non-negative equilibria as follows:

- Disease free equilibrium $E_0(\overline{T}, 0, \frac{A}{d}, 0)$, where $\overline{T} = T_0 + \frac{pA}{\alpha_0 d}$.
- Carrier free equilibrium $E_1(\hat{T}, \hat{Y}, \hat{N}, 0)$, where $\hat{T} = T_0 + \left(\frac{p}{\alpha_0}\right)\left(\frac{\beta A+\alpha(\nu+\alpha+d)}{\beta(\alpha+d)}\right)$, $\hat{Y} = \frac{\beta A - d(\nu+\alpha+d)}{\beta(\alpha+d)}$ and $\hat{N} = \frac{\beta A+\alpha(\nu+\alpha+d)}{\beta(\alpha+d)}$.

  The feasibility of this equilibrium depends on the basic reproduction number, $R_0 = \dfrac{\beta A}{(\nu+\alpha+d)d} > 1$.
- Endemic equilibrium $E^*(T^*, Y^*, N^*, C^*)$, which exist in $\hat{\Omega}$ (a subset of Ω) given by

$$\hat{\Omega} = \{(T, Y, N, C) \in \mathbb{R}^4_+ : T_0 \le T \le T_m, 0 \le Y \le \frac{A}{\alpha+d}, 0 < N \le \frac{A}{d}, 0 \le C \le C_m\}.$$

The existence of equilibrium $E_0(\overline{T}, \frac{A}{d}, 0, 0)$ is obvious. Now, existence of equilibrium E_1 can be derived by solving the set of equations below;

$$pN - \alpha_0(T - T_0) = 0, \tag{4.1}$$

$$\beta(N - Y)Y + \lambda\frac{C(N - Y)}{m + C} - (\nu + \alpha + d)Y = 0, \tag{4.2}$$

$$A - dN - \alpha Y = 0, \tag{4.3}$$

$$r(T)C - r_0\frac{C^2}{k(N)} - r_2C = 0. \tag{4.4}$$

If $C = 0$ and $Y \neq 0$ then from equation (4.2), we have

$$\beta(N - Y) - (\nu + \alpha + d) = 0. \tag{4.5}$$

From equation (4.3), we have

$$Y = \frac{A - dN}{\alpha}. \tag{4.6}$$

Thus, using equation (4.6) in (4.5), we get

$$N = \frac{A}{\alpha + d} + \frac{\alpha(\nu + \alpha + d)}{\beta(\alpha + d)} = \frac{\beta A + \alpha(\nu + \alpha + d)}{\beta(\alpha + d)} = \hat{N}(say). \tag{4.7}$$

Thus, we have from equation (4.6) and (4.7):

$$Y = \frac{A - d\hat{N}}{\alpha} = \frac{\beta A - (\nu + \alpha + d)d}{\beta(\alpha + d)} = \hat{Y}(say), \tag{4.8}$$

which exists if $\beta A - d(\nu + \alpha + d) > 0$ i.e., $R_0 = \dfrac{\beta A}{d(\nu + \alpha + d)} > 1$.

Now, from equation (4.1) and (4.7), we have

$$T = T_0 + \frac{p(\beta A + \alpha(\nu + \alpha + d))}{\alpha_0\beta(\alpha + d)} = T_0 + \frac{p\hat{N}}{\alpha_0} = \hat{T}(say).$$

Thus, the equilibrium point $E_1(\hat{T}, \hat{Y}, \hat{N}, 0)$ exists provided $R_0 > 1$. Now, the existence of equilibrium point $E^*(T^*, Y^*, N^*, C^*)$ in a subset of Ω is obtained by solving the following equations (4.1) to (4.4). We get from equation (4.4)

$$C = \frac{(r(T) - r_2)k(N)}{r_0}. \tag{4.9}$$

From equation (4.3), we have

$$N = \frac{A - \alpha Y}{d}. \tag{4.10}$$

Also from equation (4.1), we have

$$T = T_0 + \frac{pN}{\alpha_0}. \tag{4.11}$$

Using equation (4.10) in equation (4.11), we get

$$T = T_0 + \frac{p(A - \alpha Y)}{\alpha_0 d}. \tag{4.12}$$

Using equations (4.10) and (4.12) in equation (4.9), we have

$$C = \frac{\{r(T_0 + \frac{p(A-\alpha Y)}{\alpha_0 d}) - r_2\}\{k(\frac{A-\alpha Y}{d})\}}{r_0} = L(Y)(let). \tag{4.13}$$

Using equations (4.10) and (4.13) in equation (4.2), we have

$$\beta\frac{\{A - (\alpha + d)Y\}}{d}Y + \lambda\frac{\{A - (\alpha + d)Y\}L(Y)}{d(m + L(Y))} - (\nu + \alpha + d)Y = 0 = f(Y). \tag{4.14}$$

From equation (4.14), we easily observe that

$$f(0) = \frac{\lambda AL(0)}{d(m + L(0))}, \tag{4.15}$$

From equation (4.13),

$$L(0) = \frac{\{r(T_0 + \frac{pA}{\alpha_0 d}) - r_1\}\{k(\frac{A}{d})\}}{r_0} > 0,$$

so from equation (4.15), get

$$f(0) > 0,\ f(\frac{A}{\alpha + d}) = -\frac{(\nu + \alpha + d)A}{\alpha + d} < 0. \tag{4.16}$$

And differentiating equation (4.14) with respect to Y, we get

$$f'(Y) = \frac{\beta A}{d} - \frac{2\beta(\alpha + d)Y}{d} - (\nu + \alpha + d)$$
$$+\frac{\lambda}{d}\left\{\frac{(m + L(Y))\{\{A - (\alpha + d)Y\}L'(Y) - (\alpha + d)L(Y)\} - \{A - (\alpha + d)Y\}L(Y)L'(Y)}{(m + L(Y))^2}\right\},$$

Multiply by Y, then

$$Yf'(Y) = -\frac{\beta(\alpha + d)Y^2}{d} - \frac{\lambda A L(Y)}{d(m + L(Y))} + \frac{\lambda m}{d}\left\{\frac{\{A - (\alpha + d)Y\}YL'(Y)}{(m + L(Y))^2}\right\}, \tag{4.17}$$

where

$$L'(Y) = -\frac{\alpha k_1}{r_0 d}\left\{r\{T_0 + \frac{p(A - \alpha Y)}{\alpha_0 d}\} - r_2\right\} - \frac{\alpha r_1 p}{\alpha_0 r_0 d}\left\{k\left(\frac{A - \alpha Y}{d}\right)\right\}.$$

Using the value of $L'(Y)$ in equation (4.17), we get

$$Yf'(Y) < 0. \tag{4.18}$$

Consequently, since $f'(Y) < 0$ for all $Y > 0$, a unique root Y^* exists such that $0 < Y < \frac{A}{(\alpha+d)}$. Utilizing Y^*, the variables N^*, C^* and T^* are determined from equations (4.9), (4.10) and (4.11) respectively. Therefore, the endemic equilibrium $E^*(T^*, Y^*, N^*, C^*)$ exists in $\hat{\Omega}$.

Remark 4.1. *It is observed that* $\frac{dY^*}{dr_1} > 0$, $\frac{dC^*}{dr_1} > 0$, $\frac{dY^*}{dk_1} > 0$, *and* $\frac{dC^*}{dk_1} > 0$. *These expressions indicate that both the infected human population and the carrier population increase with higher values of the intrinsic growth rate coefficient and the carrying capacity increment coefficient, which are influenced by the rise in global average temperature and human activities. Furthermore, the inequalities* $\frac{dY^*}{dp} > 0$ *and* $\frac{dC^*}{dp} > 0$ *reveal that as the rate of increase in global temperature driven by anthropogenic activities grows, there is a corresponding rise in the equilibrium levels of infected individuals and carrier population density.*

5 Stability analysis

In this section, we analyze the stability behavior of the equilibria E_0, E_1 and E^*. Consider, an equilibrium is locally stable if solutions starting close to it converge to it. The local stability of E_0 and E_1 assess with the help of Jacobian matrix method [22, 25] that corresponds to the model system (2.2).

5.1 Local stability analysis

For the local stability of equilibrium point E_0 and E_1, we check the sign of eigenvalues of the Jacobian matrix. For the non-trivial endemic equilibrium E^*, we determine local stability using Routh-Hurwitz criterion [10]. The Jacobian matrix of system model (2.2) is given by

$$M = \begin{bmatrix} -\alpha_0 & 0 & p & 0 \\ 0 & \left(-\beta Y - \frac{\lambda C N}{Y(m+C)}\right) & \left(\beta Y + \frac{\lambda C}{(m+C)}\right) & \frac{\lambda m(N-Y)}{(m+C)^2} \\ 0 & -\alpha & -d & 0 \\ r_1 C & 0 & \frac{r_0 k_1 C^2}{k(N)^2} & \left(r(T) - \frac{2r_0 C}{k(N)} - r_2\right) \end{bmatrix}.$$

Consider $M(E_0)$ as Jacobian matrix of the system (2.2), evaluated at the equilibrium point E_0. Thus, $M(E_0)$ has two eigenvalues $-\alpha_0$ and $-d$, which are always negative and if $r(T_0 + \frac{pA}{\alpha_0 d}) - r_2 < 0$ and one eigenvalue is $(\nu + \alpha + d)(R_0 - 1) > 0$, which is positive and negative if $R_0 > 1$ and $R_0 < 1$. Thus, $E_0(T_0 + \frac{pA}{\alpha_0 d},\ 0,\ \frac{A}{d},\ 0)$ is unstable and stable if $R_0 > 1$ and $R_0 < 1$, respectively. Similarly, for equilibrium $E_1(\bar{T},\ \bar{Y},\ \bar{N},\ 0)$ the matrix $M(E_1)$ has one positive eigenvalue $(r(\bar{T}) - r_2)$, when endemic equilibrium exists. Thus, equilibrium $E_1(\bar{T},\ \bar{Y},\ \bar{N},\ 0)$is unstable. In additional, we use the Routh-Hurwitz criterion to study the local stability behavior of non-trivial equilibrium $E^*(T^*, Y^*, N^*, C^*)$, which is outlined in the theorem.

***Theorem* 5.1** *States that, under the following conditions, the equilibrium* $E^*(T^*, Y^*, N^*, C^*)$ *is locally asymptotically stable,*

$$(a_1a_2 - a_3)a_3 - a_1^2a_4 > 0, \tag{5.1}$$

where,

$$\begin{aligned}
a_1 =&\alpha_0 + d + \left\{\beta Y^* + \frac{\lambda C^*N^*}{Y^*(m+C^*)}\right\} + \frac{r_0C^*}{k(N^*)},\\
a_2 =&\alpha_0\left\{d + \beta Y^* + \frac{\lambda C^*N^*}{Y^*(m+C^*)} + \frac{r_0C^*}{k(N^*)}\right\} + \frac{r_0C^*}{k(N^*)}\left\{d + \beta Y^* + \frac{\lambda C^*N^*}{Y^*(m+C^*)}\right\}\\
&+ d\left\{\beta Y^* + \frac{\lambda C^*N^*}{Y^*(m+C^*)}\right\} + \alpha\left\{\beta Y^* + \frac{\lambda C^*}{(m+C^*)}\right\},\\
a_3 =&\alpha_0\left\{\frac{r_0C^*}{k(N^*)}\left\{d + \beta Y^* + \frac{\lambda C^*N^*}{Y^*(m+C^*)}\right\} + d\left\{\beta Y^* + \frac{\lambda C^*N^*}{Y^*(m+C^*)}\right\}\right\}\\
&+ \alpha_0\alpha\left\{\beta Y^* + \frac{\lambda C^*}{(m+C^*)}\right\} + \frac{dr_0C^*}{k(N^*)}\left\{\beta Y^* + \frac{\lambda C^*N^*}{Y^*(m+C^*)}\right\}\\
&+ \alpha\left\{\beta Y^* + \frac{\lambda C^*}{(m+C^*)}\right\}\frac{r_0C^*}{k(N^*)} + \frac{\alpha r_0k_1C^{*2}}{k(N^*)^2}\left\{\frac{\lambda m(N^*-Y^*)}{(m+C^*)^2}\right\},\\
a_4 =&\alpha r_1pC^*\left\{\frac{\lambda m(N^*-Y^*)}{(m+C^*)^2}\right\} + \frac{\alpha\alpha_0r_0k_1C^{*2}}{k(N^*)^2}\left\{\frac{\lambda m(N^*-Y^*)}{(m+C^*)^2}\right\}\\
&+ \alpha_0\left\{(\alpha+d)\beta Y^* + \frac{d\lambda C^*N^*}{Y^*(m+C^*)} + \frac{\alpha\lambda C^*}{(m+C^*)}\right\}\frac{r_0C^*}{k(N^*)}.
\end{aligned}$$

Here, it is noted that $a_i > 0$, for all $i = 1, 2, 3, 4$.
Proof: See the Appendix 1.

5.2 Global stability analysis

To the global stability analysis, using Lyapunov's direct method to evaluate the stability of endemic equilibrium $E^*(T^*,\ Y^*,\ N^*,\ C^*)$ for long term behavior, is outlined in subsequent theorem.

***Theorem* 5.2.** *If the following criteria are satisfied, the equilibrium* E^* *is globally asymptotically stable in* $\hat{\Omega}$*,*

$$\lambda^2\alpha {C_m}^2 < \beta^2 d(m + C_m)^2 {Y_m}^2, \tag{5.2}$$

and

$$4pr_1k_1\alpha\lambda^2m^2k(\frac{A}{d})C^*N^{*2} < \alpha_0r_0d\beta_2{Y_m}^2(m + C_m)k(N^*)(m + C^*)^2. \tag{5.3}$$

where,
Y_m *and* C_m *are the maximum value of* Y *and* C*, which are given by* $Y_m = \frac{A}{\alpha+d}$ *and* $C_m = \left\{\frac{(r(T_m)-r_2)k(\frac{A}{d})}{r_0}\right\}$ *for* $T_m = T_0 + \frac{pA}{\alpha_0 d}$.
Proof: See the Appendix 2.

6 Numerical simulation

In this section, to visualize the dynamics of the proposed model, we present numerical simulation of the model system (2.2) corresponding to the following specified parameter values by using MATLAB [32, 40]:

With parameter values mentioned above, we get the endemic equilibrium E^* as

$$T^* = 15.20,\ N^* = 1988.92,\ Y^* = 301.11,\ C^* = 6067.34.$$

The Jacobian matrix (M_{E^*}) for the above values of parameters at $E^*(T^*, Y^*, N^*, C^*)$;

$$\begin{bmatrix} -0.1 & 0 & 0.00001 & 0\\ 0 & -0.11943 & 0.02319 & 0.0006758\\ 0 & -0.1 & -0.01 & 0\\ 6.06734 & 0 & 0.146876 & -0.054198 \end{bmatrix},$$

which corresponds to following eigenvalues of the Jacobian matrix

Table* 6.1: Values of the parameters used in model system* (2).

Parameter	*Description*	*Value*
p	Growth rate coefficient of average global temperature from anthropogenic sources	0.00001
α_0	Natural depletion rate coefficient of average global temperature	0.1
T_0	Global average temperature of pre-industrial era	15
A	Rate of constant immigration and birth in the consider region	50
β	Transmission coefficient due to infective population	0.00002
λ	Transmission coefficient due to carrier population	0.02
ν	Recovery rate of coefficient of infective population	0.02
d	Natural death rate constant of human population	0.01
α	Disease related death rate coefficient of infective population	0.1
m	Half saturation point at which the transmission rate becomes half	1000
r_0	Intrinsic growth rate coefficient of carrier population	0.04
r_1	Increment coefficient of intrinsic growth rate due to temperature	0.001
k_0	Carrying capacity of carrier population	500
k_1	Increment coefficient of carrying capacity due to anthropogenic activities	2
r_2	Carrier population depletes due to various unfavorable environmental factors	0.001

$$-0.0997, -0.0953, \text{ and } -0.0443 \pm 0.0121i.$$

Negative real part sign of all the eigenvalues confirms that the equilibrium E^* is locally asymptotically stable. In Figure 6.1, the solution trajectories in the $N - Y - C$ space are shown for four different initial conditions. All trajectories converge towards the equilibrium point E^*, clearly demonstrating its global stability. The computer generated three-dimensional plot of N versus Y versus C for model system (2.2), corresponding to the initial points [15,200,3800,5800] [15,1300,1800,500], [15,1450,2200,4200] and [15,180,3500,2800] further confirms this result. The trajectories from each initial condition move toward the endemic equilibrium $E^*(T^*, Y^*, N^*, C^*)$, illustrating that the system eventually stabilizes at an endemic equilibrium state irrespective of the starting values. This consistent convergence in the $N - Y - C$ phase space verifies the global stability of the endemic equilibrium.

Figure 6.2 illustrates the temporal variation of global average temperature $T(t)$ over time (in days) for three different values of the anthropogenic activity parameter $p = 0.00001,\ 0.00002$ and 0.00003. It is observed that as the value of p increases, the corresponding temperature rises more rapidly and attains a higher equilibrium level. The curves show an initial steep increase in temperature followed by stabilization, indicating that anthropogenic activities significantly accelerate temperature elevation before reaching a steady-state value. Specifically, higher values of p (represented by the green curve) lead to a greater and faster temperature rise compared to lower values (blue and red curves). This behavior demonstrates the direct influence of anthropogenic factors on the long-term warming trend of the global environment. Furthermore in figure 6.3, All variables exhibit a rapid increase during the initial phase followed by stabilization, signifying that the system eventually attains equilibrium. The synchronized approach of these variables toward steady states reflects the internal consistency and stability of the proposed model, emphasizing the interconnected effects of temperature rise, infection spread, and carrier population dynamics. Figure 6.4 depicts the effect of varying the increased temperature-dependent growth rate due to anthropogenic activities parameter (r_1) on infective and carrier populations. Both populations rise rapidly at the beginning and eventually stabilize, indicating equilibrium. Higher values of r_1 result in faster growth and larger steady-state levels, showing that increased temperature accelerates and carrier proliferation and infection spread. Figures 6.5 and 6.6 illustrate the effects of the increased carrying capacity coefficient of carriers due to anthropogenic activities (k_1) and the immigration rate by birth and outside in the consider region A on the densities of infective human and carrier population. Both k_1 and A, when increased, cause a rise in infected individuals and carrier population. Figure 6.7 verifies that an increase in the carrier population growth rate (r_0) results in elevated densities of both infective and carrier populations.

The surface plots in Figures (6.8)-(6.10) illustrate the combined effects of different model parameters on

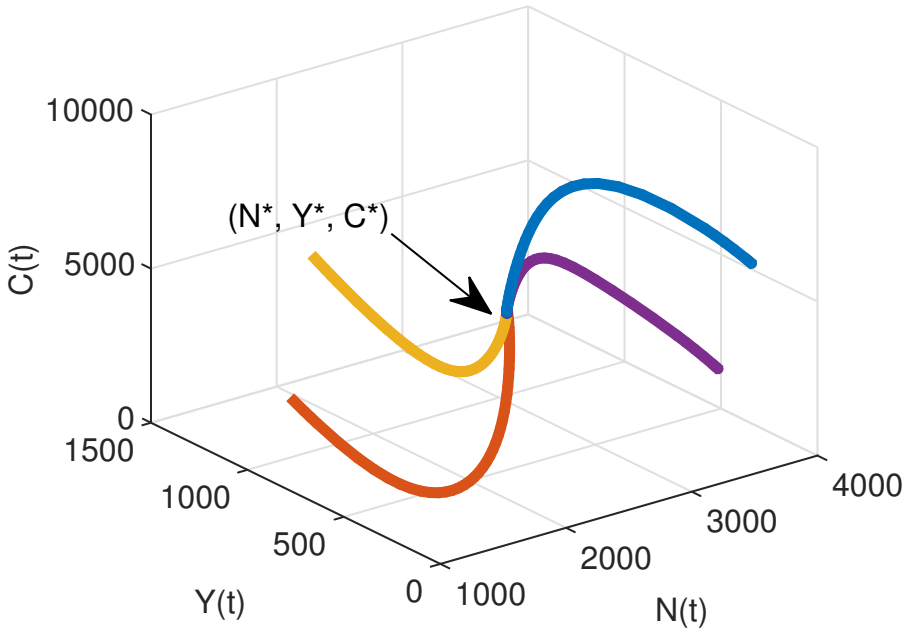

***Figure* 6.1:** *Global stability plot of endemic equilibrium E^* in $N - Y - C$ space.*

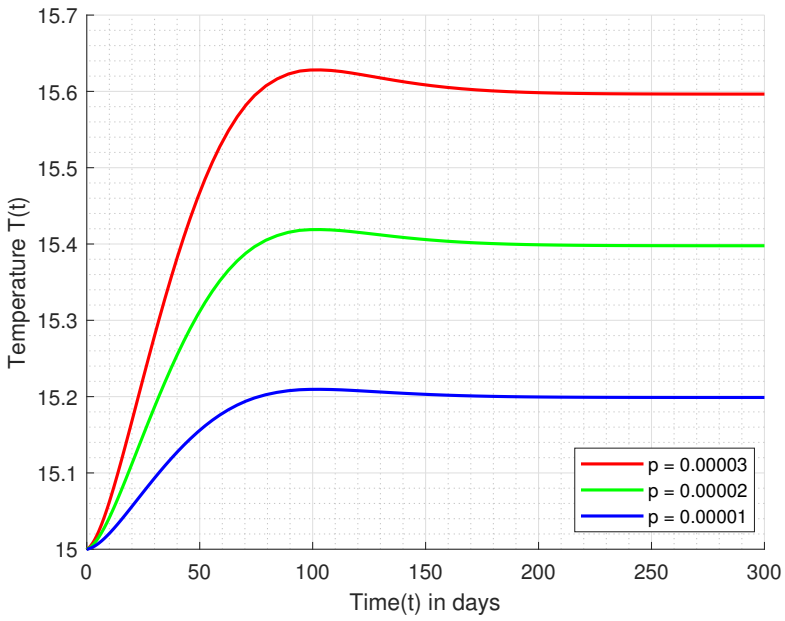

***Figure* 6.2:** *Variation of global average temperature over time (in days) under different levels of anthropogenic activity (p).*

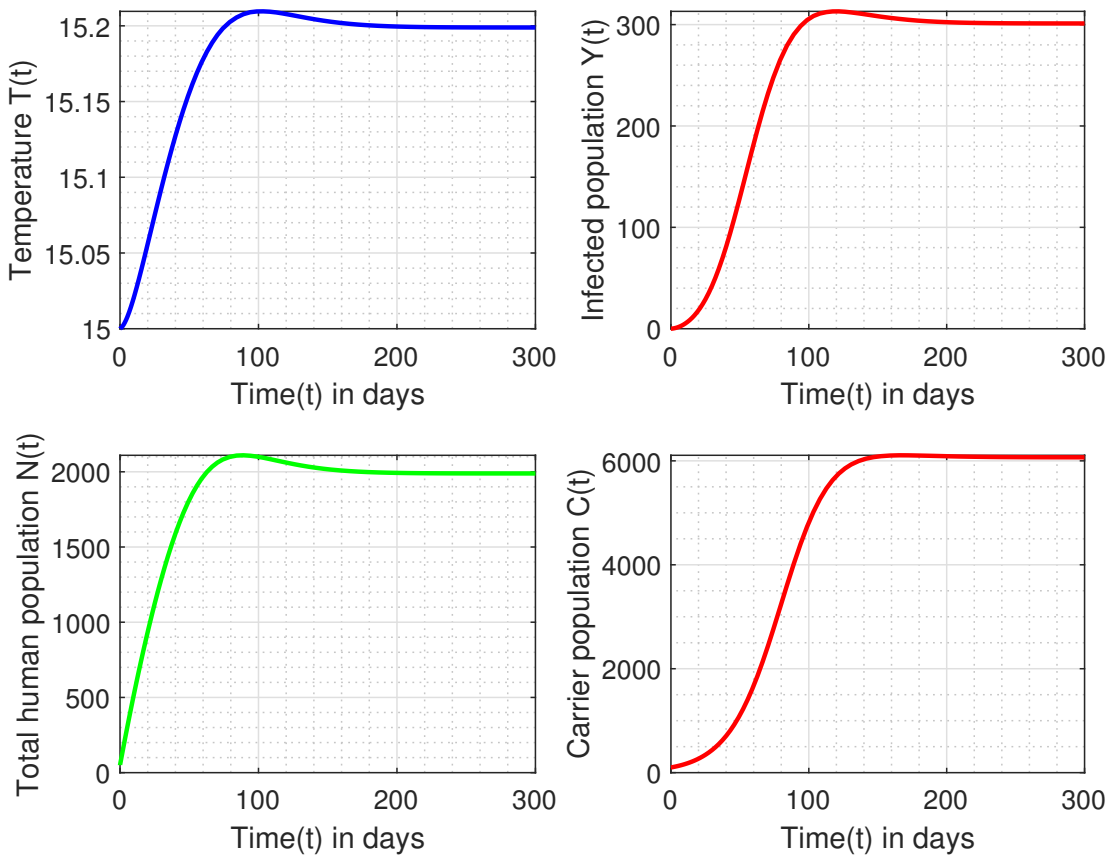

***Figure* 6.3:** *Temporal variation of dynamical variables; global average temperature* (T)*, infected population* (Y)*, human population* (N)*, and carrier population* (C)*.*

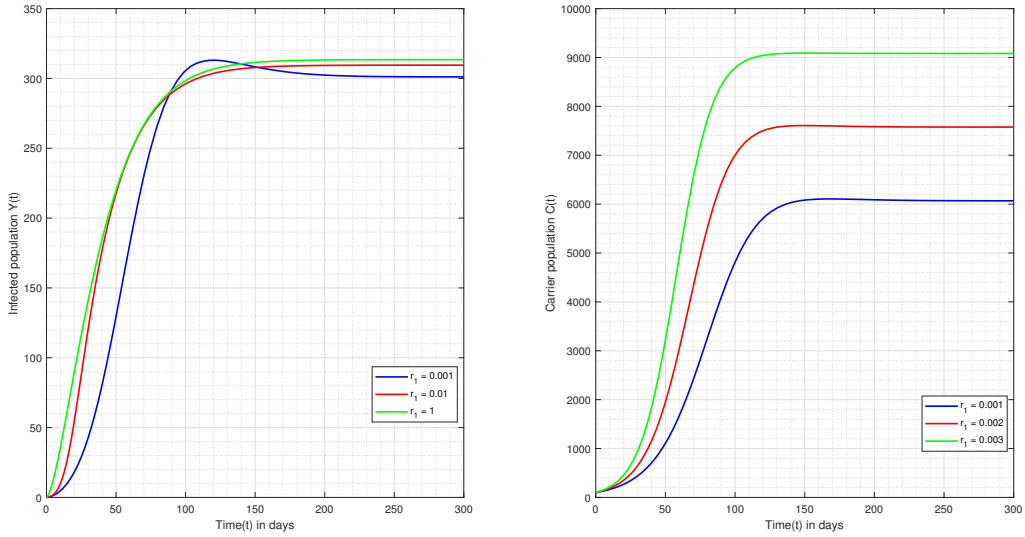

***Figure* 6.4:** *Variations in infected and carrier population with different parameter values* $r_1 = \{0.001, 0.01, 1\}$ *and* $r_1 = \{0.001, 0.002, 0.003\}$.

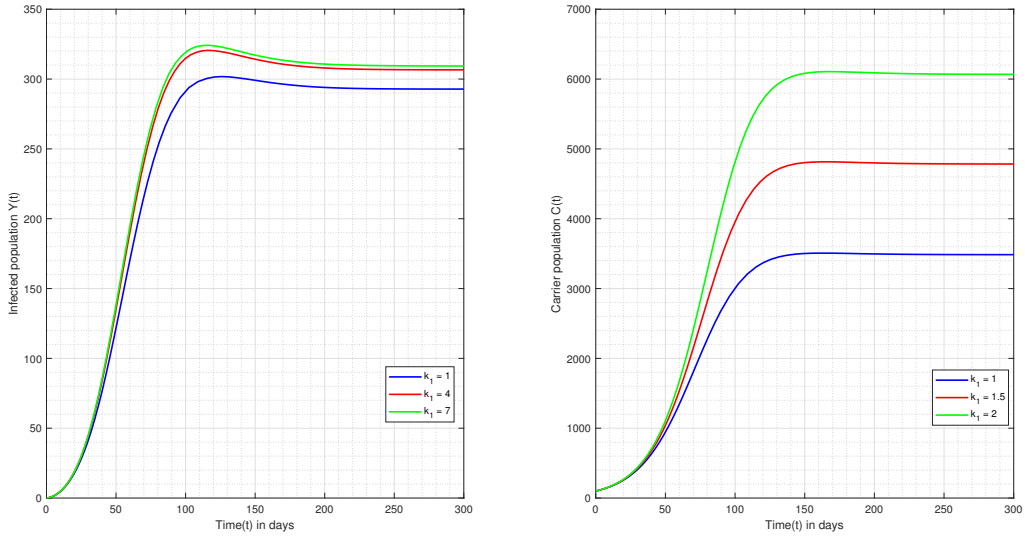

***Figure* 6.5:** *Variations in infected and carrier population with different parameter values of* $k_1 = \{1, 4, 7\}$ *and* $k_1 = \{1, 1.5, 2\}$.

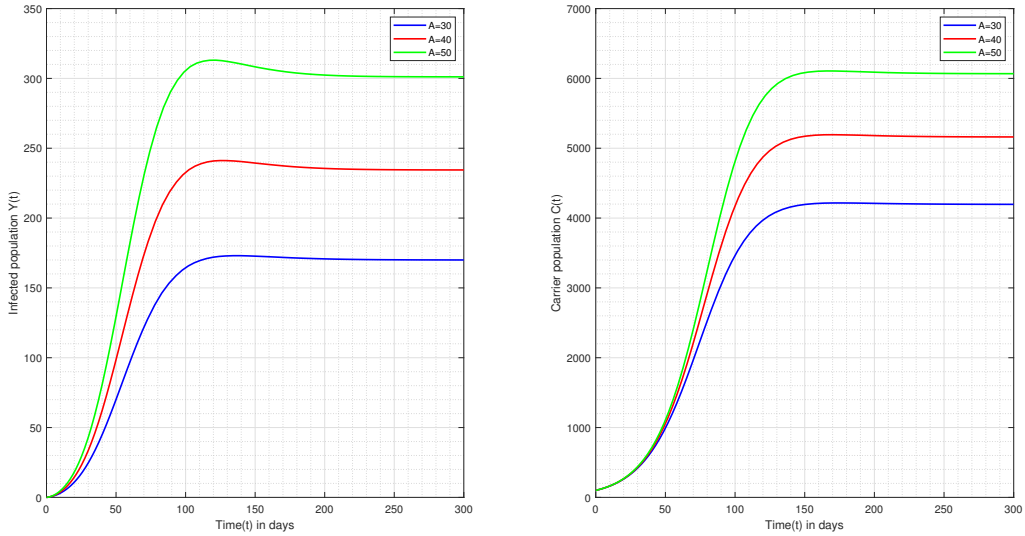

***Figure* 6.6:** *Variations in infected and carrier population with different parameter values of* $A = \{30, 40, 50\}$.

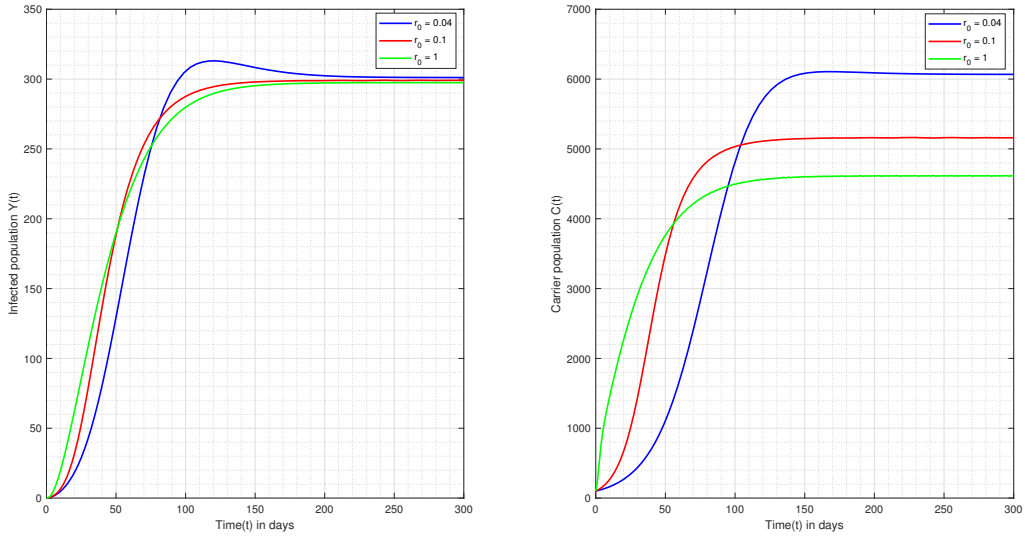

***Figure* 6.7:** *Variations in infected and carrier population with different parameter values of* $r_0 = \{0.04, 0.1, 1\}$.

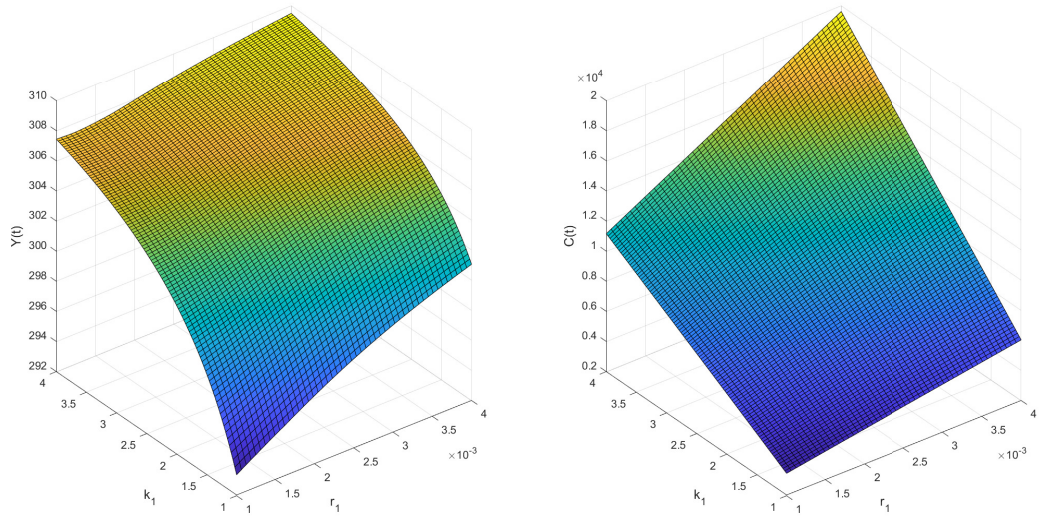

Figure* 6.8: Surface plots of equilibrium levels of infected and carrier population based on r_1, and k_1, while maintaining same values for other parameter as in Table 6.1.*

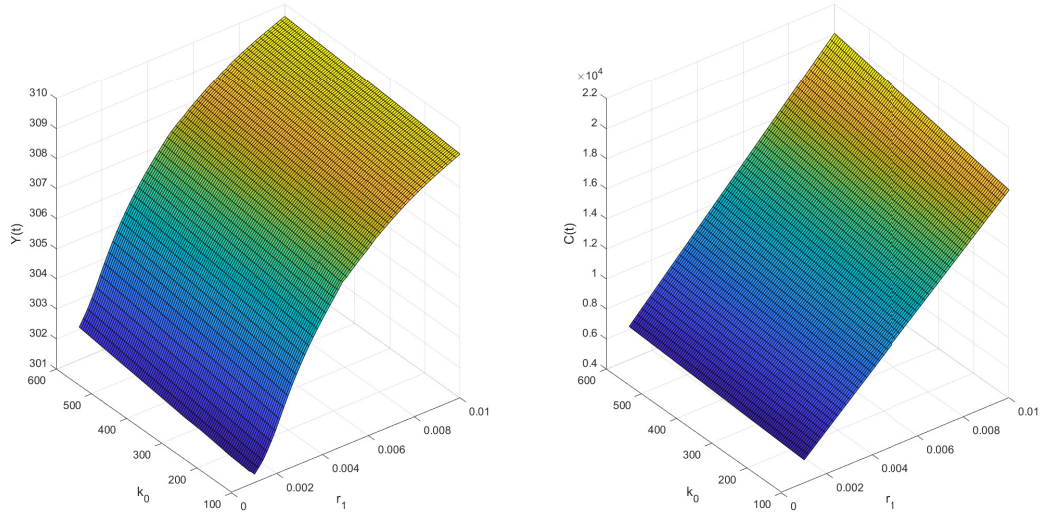

Figure* 6.9: Surface plots of equilibrium levels of infected and carrier population based on r_1, and k_0, while maintaining same values for other parameter as in Table 6.1.*

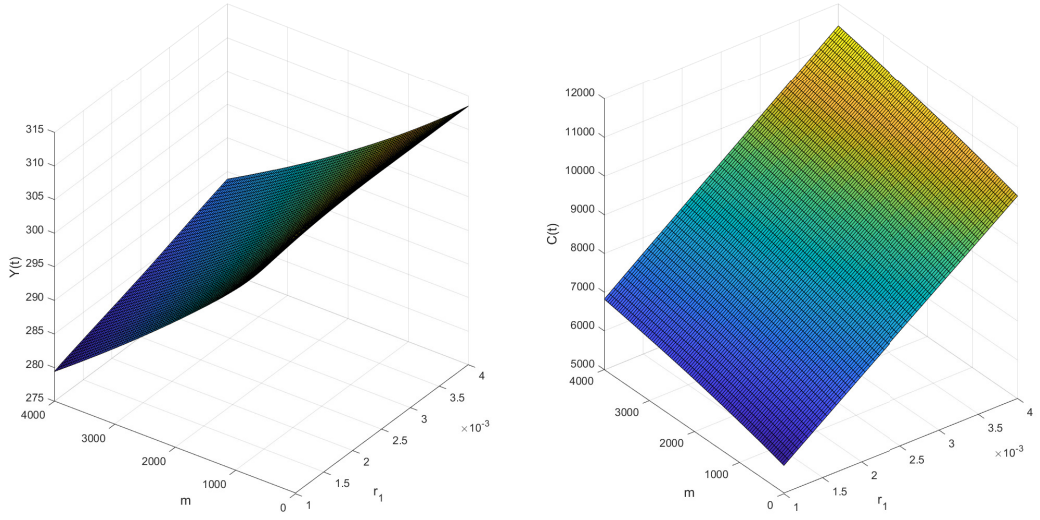

Figure* 6.10: Surface plots of equilibrium levels of infected and carrier population based on r_1, and m, while maintaining same values for other parameter as in Table 6.1.*

the infected human population $Y(t)$ and carrier population $C(t)$. In Figure 6.8, an increase in the intrinsic growth rate coefficient (r_1) and increment factor of carrying capacity (k_1), both influenced by global average temperature and anthropogenic activities, leads to a noticeable rise in both $Y(t)$ and $C(t)$, showing that stronger growth dynamics promote disease spread. Figure 6.9 depicts a similar pattern when (r_1) and the carrying capacity (k_0) increase, highlighting how environmental capacity amplifies infection persistence. Finally, Figure 6.10 shows that higher values of (r_1) and the half-saturation constant (m), which represents the rate of resource absorption at half its maximum, further elevate $Y(t)$ and $C(t)$. These results collectively emphasize that human-induced changes in biological and environmental parameters can significantly intensify the disease transmission potential through carrier populations.

7 Conclusions

The accelerating rise in global temperature projected to increase by 2°C to 4°C by 2050 poses a profound threat to public health by reshaping the dynamics of food-borne diseases. Even a modest warming significantly alters pathogen behavior, accelerates replication rates, enhances virulence, and expands the geographical range of disease carrying insects such as houseflies. These climatic shifts intensify the risk of outbreaks caused by pathogens like Salmonella typhi, underscoring the urgent need to understand and mitigate temperature-driven disease transmission.

This study presents a nonlinear mathematical model to investigate the impact of anthropogenic temperature rise on the transmission dynamics of carrier-dependent infectious diseases. The model incorporates four key variables: global temperature, susceptible and infected human populations, and the carrier population, while accounting for temperature-dependent carrier growth and human population dependent carrying capacity. Analytical and numerical approaches were employed to examine how temperature variations, induced by human activities, influence disease spread through their effect on carrier density. The model exhibits three non-negative equilibria: a carrier-free equilibrium, a carrier-disease-free equilibrium, and an interior (endemic) equilibrium. Stability analysis reveals that both boundary equilibria are unstable, indicating that disease eradication is difficult once carriers are introduced into the environment. Local and global stability of the interior equilibrium were examined using the Routh-Hurwitz criterion and Lyapunov's direct method, respectively. The results show that a rise in temperature enhances the intrinsic growth rate of the carrier population, leading to an increase in infection prevalence among humans. Thus, temperature-induced carrier proliferation has a destabilizing effect on the overall disease dynamics.

Numerical simulations support the analytical findings, illustrating that increasing global temperature

significantly raises carrier density and consequently the number of infected individuals. This positive association emphasizes the role of environmental factors in shaping epidemic patterns. Improper waste disposal, open drainage systems, and poor sanitation further exacerbate the problem by providing ideal breeding sites for carriers, which amplifies infection transmission rates. Overall, the study concludes that climate change, resulting from anthropogenic factors, amplifies carrier population growth and consequently escalates the number of infections. Even moderate temperature increases can significantly influence disease dynamics by enhancing pathogen survival, accelerating life cycles, and extending the geographical range of disease vectors. Hence, effective environmental management and climate adaptive public health strategies are essential to control the future burden of food-borne diseases in a warming world.

***Appendix* 1. *Proof of the Theorem* 5.1**

Proof: The Jacobian matrix for the model system (2.2);

$$M_{E^*} = \begin{bmatrix} -\alpha_0 & 0 & p & 0 \\ 0 & \left(-\beta Y^* - \frac{\lambda C^* N^*}{Y^*(m+C^*)}\right) & \left(\beta Y^* + \frac{\lambda C^*}{(m+C^*)}\right) & \frac{\lambda m(N^*-Y^*)}{(m+C^*)^2} \\ 0 & -\alpha & -d & 0 \\ r_1 C^* & 0 & \frac{r_0 k_1 C^{*2}}{k(N^*)^2} & -\frac{r_0 C^*}{k(N^*)} \end{bmatrix}.$$

Suppose that λ is the eigen value of the matrix M_E^*. The eigen function is given by

$$\lambda^4 + a_1\lambda^3 + a_2\lambda^2 + a_3\lambda + a_4 = 0. \tag{7.1}$$

Where

$$\begin{aligned}
a_1 =& \alpha_0 + d + \left\{\beta Y^* + \frac{\lambda C^* N^*}{Y^*(m+C^*)}\right\} + \frac{r_0 C^*}{k(N^*)}, \\
a_2 =& \alpha_0 \left\{d + \beta Y^* + \frac{\lambda C^* N^*}{Y^*(m+C^*)} + \frac{r_0 C^*}{k(N^*)}\right\} + \frac{r_0 C^*}{k(N^*)} \left\{d + \beta Y^* + \frac{\lambda C^* N^*}{Y^*(m+C^*)}\right\} \\
& + d\left\{\beta Y^* + \frac{\lambda C^* N^*}{Y^*(m+C^*)}\right\} + \alpha\left\{\beta Y^* + \frac{\lambda C^*}{(m+C^*)}\right\}, \\
a_3 =& \alpha_0 \left\{\frac{r_0 C^*}{k(N^*)}\left\{d + \beta Y^* + \frac{\lambda C^* N^*}{Y^*(m+C^*)}\right\} + d\left\{\beta Y^* + \frac{\lambda C^* N^*}{Y^*(m+C^*)}\right\}\right\} \\
& + \alpha_0\alpha\left\{\beta Y^* + \frac{\lambda C^*}{(m+C^*)}\right\} + \frac{d r_0 C^*}{k(N^*)}\left\{\beta Y^* + \frac{\lambda C^* N^*}{Y^*(m+C^*)}\right\} \\
& + \alpha\left\{\beta Y^* + \frac{\lambda C^*}{(m+C^*)}\right\}\frac{r_0 C^*}{k(N^*)} + \frac{\alpha r_0 k_1 C^{*2}}{k(N^*)^2}\left\{\frac{\lambda m(N^*-Y^*)}{(m+C^*)^2}\right\}, \\
a_4 =& \alpha r_1 p C^*\left\{\frac{\lambda m(N^*-Y^*)}{(m+C^*)^2}\right\} + \frac{\alpha\alpha_0 r_0 k_1 C^{*2}}{k(N^*)^2}\left\{\frac{\lambda m(N^*-Y^*)}{(m+C^*)^2}\right\} \\
& + \alpha_0\left\{(\alpha+d)\beta Y^* + \frac{d\lambda C^* N^*}{Y^*(m+C^*)} + \frac{\alpha\lambda C^*}{(m+C^*)}\right\}\frac{r_0 C^*}{k(N^*)}.
\end{aligned}$$

Using the Routh-Hurwitz criterion, the equilibrium $E_3(T^*, Y^*, N^*, C^*)$ in Eq. (32) is locally asymp-totically stable, provided that the following conditions are satisfied

$$(a_1a_2 - a_3)a_3 - a_1^2 a_4 > 0.$$

for all $a_i > 0$, for all $i = 1, 2, 3, 4$.

***Appendix* 2. *Proof of the Theorem* 5.2**

Proof: For the proof of this theorem, we use Lyapunov direct method. For this first, we let the following positive definite Lyapunov function

$$V = \frac{L_0}{2}(T - T^*)^2 + L_1(Y - Y^* - Y^* log\frac{Y}{Y^*}) + \frac{L_2}{2}(N - N^*)^2 + L_3(C - C^* - C^* log\frac{C}{C^*}). \tag{7.2}$$

Differentiating equation (7.2) with respect to t, we get

$$\frac{dV}{dt} = L_0(T - T^*)\dot{T} + L_1(Y - Y^*)\frac{\dot{Y}}{Y} + L_2(N - N^*)\dot{N} + L_3(C - C^*)\frac{\dot{C}}{C}. \tag{7.3}$$

From model system (2.2), we have

$$\dot{T} = p(N - N^*) - \alpha_0(T - T^*), \tag{7.4}$$

$$\frac{\dot{Y}}{Y} = -\left\{\beta + \frac{\lambda C^* N^*}{YY^*(m + C^*)}\right\}(Y - Y^*) + \left\{\beta + \frac{\lambda C}{Y(m + C)}\right\}(N - N^*) - \frac{\lambda m(Y - N^*)}{Y(m + C)(m + C^*)}(C - C^*), \tag{7.5}$$

$$\dot{N} = -d(N - N^*) - \alpha(Y - Y^*), \tag{7.6}$$

$$\frac{\dot{C}}{C} = r_1(T - T^*) - \frac{r_0}{k(N)}(C - C^*) + \frac{r_0 k_1 C^*}{k(N)k(N^*)}(N - N^*). \tag{7.7}$$

Using equations (7.4) to (7.7) in equation (7.3), we get

$$\begin{aligned}
\dot{V} =& L_0\left\{p(N - N^*) - \alpha_0(T - T^*)\right\}(T - T^*) \\
&+ L_1\left\{\left(\beta + \frac{\lambda C}{Y(m + C)}\right)(N - N^*) - \left(\beta + \frac{\lambda C^* N^*}{YY^*(m + C^*)}\right)(Y - Y^*)\right\}(Y - Y^*) \\
&- L_1\left\{\frac{\lambda m(Y - N^*)}{Y(m + C)(m + C^*)}(C - C^*)\right\}(Y - Y^*) \\
&+ L_2\{-d(N - N^*) - \alpha(Y - Y^*)\}(N - N^*) \\
&+ L_3\left\{r_1(T - T^*) - \frac{r_0(C - C^*)}{k(N)} + \frac{r_0 k_1 C^*(N - N^*)}{k(N)k(N^*)}\right\}(C - C^*), \\
\dot{V} =& -\left\{\frac{L_0\alpha_0}{2}(T - T^*)^2 - L_0 p(N - N^*)(T - T^*) + \frac{dL_2}{4}(N - N^*)^2\right\} \\
&+ \{(L_1\beta - \alpha L_2)(Y - Y^*)(N - N^*)\} \\
&- \left\{\frac{L_1\beta}{2}(Y - Y^*)^2 - \frac{\lambda m N^* L_1}{Y(m + C)(m + C^*)}(C - C^*)(Y - Y^*) + \frac{r_0 L_3}{2k(N)}(C - C^*)^2\right\} \\
&- \left\{\frac{\lambda m L_1}{(m + C)(m + C^*)}\right\}(C - C^*)(Y - Y^*) - \left\{\frac{\lambda L_1 C^* N^*}{YY^*(m + C^*)}\right\}(Y - Y^*)^2 \\
&- \left\{\frac{dL_2}{2}(N - N^*)^2 - \frac{L_1\lambda C}{Y(m + C)}(N - N^*)(Y - Y^*) + \frac{L_1\beta}{2}(Y - Y^*)^2\right\} \\
&- \left\{\frac{r_0 L_3}{4k(N)}(C - C^*)^2 - \frac{L_3 r_0 k_1 C^*}{k(N)k(N^*)}(N - N^*)(C - C^*) + \frac{dL_2}{4}(N - N^*)^2\right\} \\
&- \left\{\frac{r_0 L_3}{4k(N)}(C - C^*)^2 - r_1 L_3(T - T^*)(C - C^*) + \frac{L_0\alpha_0}{2}(T - T^*)^2\right\},
\end{aligned}$$

we take the constants $L_1 = \frac{\alpha}{\beta}$. and $L_2 = 1$, such that $(L_1\beta - \alpha L_2 = 0)$, we have

$$\begin{aligned}
\dot{V} =& -\left\{\frac{L_0\alpha_0}{2}(T - T^*)^2 - L_0 p(N - N^*)(T - T^*) + \frac{dL_2}{4}(N - N^*)^2\right\} \\
&- \left\{\frac{L_1\beta}{2}(Y - Y^*)^2 - \frac{\lambda m N^* L_1}{Y(m + C)(m + C^*)}(C - C^*)(Y - Y^*) + \frac{r_0 L_3}{2k(N)}(C - C^*)^2\right\} \\
&- \left\{\frac{\lambda m L_1}{(m + C)(m + C^*)}\right\}(C - C^*)(Y - Y^*) - \left\{\frac{\lambda L_1 C^* N^*}{YY^*(m + C^*)}\right\}(Y - Y^*)^2 \\
&- \left\{\frac{dL_2}{2}(N - N^*)^2 - \frac{L_1\lambda C}{Y(m + C)}(N - N^*)(Y - Y^*) + \frac{L_1\beta}{2}(Y - Y^*)^2\right\} \\
&- \left\{\frac{r_0 L_3}{4k(N)}(C - C^*)^2 - \frac{L_3 r_0 k_1 C^*}{k(N)k(N^*)}(N - N^*)(C - C^*) + \frac{dL_2}{4}(N - N^*)^2\right\} \\
&- \left\{\frac{r_0 L_3}{4k(N)}(C - C^*)^2 - r_1 L_3(T - T^*)(C - C^*) + \frac{L_0\alpha_0}{2}(T - T^*)^2\right\}.
\end{aligned}$$

Here, $\dot{V}$ is negative definite if

$$L_0 < \frac{\alpha_0 d}{2p^2},$$

$$\frac{\lambda^2 L_1 C^2}{\beta d Y^2 (m+C)^2} < L_2,$$

$\Longrightarrow$

$$\alpha\lambda^2 {C_m}^2 < d\beta^2 {Y_m}^2 (m+C_m)^2.$$

where Y_m and C_m are the maximum value of Y and C.
Now

$$\frac{\lambda^2 m^2 N^{*2} k(N)}{\beta r_0 Y^2 (m+C)^2 (m+C^*)^2} L_1 < L_3,$$

$$\frac{2{r_1}^2 {L_3}^2}{\alpha_0 r_0 L_0} < \frac{L_3}{k(N)},$$

$$\frac{L_3}{k(N)} < \frac{dk(N^*)^2}{4 r_0 {k_1}^2 C^{*2}},$$

Eliminate L_0, L_1 and L_3 from these Eqs. we get

$$\frac{\alpha\lambda^2 m^2 N^{*2} k(N)}{r_0 \beta^2 Y^2 (m+C)^2 (m+C^*)^2} < \frac{\alpha_0 d k(N^*)}{4 p r_1 k_1 C^*}.$$

So, conditions for $\dot{V}$ is negative definite

$$\alpha\lambda^2 {C_m}^2 < d\beta^2 {Y_m}^2 (m+C_m)^2,$$

and

$$\frac{\alpha k(\frac{A}{d})\lambda^2 m^2 N^{*2}}{r_0 \beta^2 {Y_m}^2 (m+C_m)^2 (m+C^*)^2} < \frac{\alpha_0 d k(N^*)}{4 p r_1 k_1 C^*}.$$

where Y_m and C_m are the maximum value of Y and C.

References

[1] R.M. Anderson and R.M. May, Population biology of infectious diseases, part-I, *Nature*, **280** (1979), 361-367.

[2] M. S. Arora, S. Singh, A. Omar and S.N. Mishra, Mathematical modelling and sensitivity analysis of effect of global warming on carrier based infectious diseases, *Jñānābha*, **52**(2) (2022), 138-152.

[3] G. Agrawal, A.K. Agrawal and J. Dhar, Effects of Human Population and Atmospheric Pollution on Rainfall: A Modeling Study, *J. Indian Math. Soc.*, **91**(3-4) (2024), 550-564.

[4] N.T. Bailey, *The Mathematical Theory of Infectious Diseases and its Applications*, 2nd ed., Griffin, London, 1975.

[5] F. Brauer and C. Castillo-Chavez, *Mathematical models in population biology and epidemiology, Texts in applied mathematics*, Springer, 2001.

[6] C.T. Codeco, Endemic and epidemic dynamics of cholera: the role of the aquatic reservoir, *BMC Infect Dis.*, **1** (2001), 1-14.

[7] S. Chaudhry, G. Agrawal, M. Martcheva and A.K. Misra, Modeling the impact of temperature on the dynamics of carrier-dependent infectious diseases with control strategies, *Math. Biosci. Eng.*, **22**(7) (2025), 1722-1750.

[8] Climate change and health: Factsheet [Internet], *World Health Organisation*, (2018). Available from: `http://www.who.int/mediacentre/factsheets/fs266/en/`

[9] O. Diekmann and J.A. Heesterbeek, *Mathematical epidemiology of infectious diseases*, Wiley series in mathematical and computational biology, Wiley, 2000.

[10] P. Das and D. Mukherjee, Qualitative Analysis of a Cholera Bacteriophage Model, *Int. Sch. Res. Notices*, **31** (2012), 621939.

[11] P.R. Epstein, Climate change and emerging infectious diseases, *Microbes Infect.*, **3**(9) (2001), 747-754.

[12] Global and European temperatures [Internet], *European Environment Agency*, (2020). Available from: `https://www.eea.europa.eu/data-and-maps/indicators/globaland-european-temperature-10/assessment`

[13] Global Warming [Internet], *Encyclopaedia Britannica, Inc.*, (2019). Available from: `https://www.britannica.com/science/global-warming`

[14] R.K. Gupta, S. Pal and A.K. Misra, Modeling the impact of precautionary measures and sanitation practices broadcasted through media on the dynamics of bacterial diseases, *Model Earth Syst Environ.*, **9** (2023), 397-412.
[15] M. Ghosh, J.B. Shukla, P. Chandra and P. Sinha, An epidemiological model for carrier dependent infectious diseases with environmental effect, *Int J Appl Sci Comput.*, **7** (2000), 188-204.
[16] H.W. Hethcote, Qualitative analysis of communicable disease models, *Math Biosci.*, **28** (1976), 335-356.
[17] K. Lata, S.N. Mishra and A.K. Misra, An optimal control problem for carrier dependent diseases, *Biosyst.*, **187** (2020), 104039.
[18] A.J. McMichael, D.H. Campbell, C.F. Corvalan, K.L. Ebi, A.K. Githeko, J.D. Scheraga and A. Woodword, *Climate change and human health-risks and responses*, World Health Organization, Geneva, (2003).
[19] A.K. Misra, S.N. Mishra, A.L. Pathak, P. Misra and R. Naresh, Modeling the effect of time delay in controlling the carrier dependent infectious disease-cholera, *Appl Math Comput.*, **218** (2012), 11547-11557.
[20] A.K. Misra, S.N. Mishra, A.L. Pathak, P.K. Srivastava and P. Chandra, A mathematical model for the control of carrier-dependent infectious diseases with direct transmission and time delay, *Chaos Soliton Fract.*, **57** (2013), 41-53.
[21] A.K. Misra, A. Gupta and E. Venturino, Modeling biological control of carrier-dependent infectious diseases, *Comput Math Methods.*, **3**(6) (2021), e1127.
[22] S.N. Mishra, Modeling the effect of ecological conditions in the habitat on the spread of tuberculosis, *Jñānābha*, **50**(2) (2020), 212-222.
[23] R. Naresh, S. Pandey and A.K. Misra, Analysis of a vaccination model for carrier dependent infectious diseases with environmental effects, *Nonlinear Anal Model.*, **13**(3) (2008), 331-350.
[24] P. Reiter, Climate change in mosquito borne disease, *Environ Health Perspect.*, **109**(1) (2001), 141-161.
[25] D.J. Rogers, and S.E. Randolf, The global spread of malaria in a future warmer world, *Science*, **289** (2000), 1763-1766.
[26] H. Sanchez-Arroyo and J.L. Capinera, *House fly, Musca domestica Linnaeus (Insecta: Diptera:Muscidae)*. Muscidae-domestica Linnaeus, (1998), `http://edis.ifas.ufl.edu/pdffiles/in/in20500.pdf`.
[27] J.B. Shukla, V. Singh and A.K. Misra, Modeling the spread of an infectious disease with bacteria and carriers in the environment, *Nonlinear Anal Real World Appl.*, **12**(5) (2011), 2541-2551.
[28] J.B. Shukla, A. Goyal, S. Singh and P. Chandra, Effects of habitat characteristics on the growth of carrier population leading to increased spread of typhoid fever: A model, *J Epidemiol Glob Health.*, **4** (2) (2014), 107-114.
[29] J.B. Shukla, M. Verma and A.K. Misra, Effect of global warming on sea level rise: A modeling study, *Ecol. Complex.*, **32** (2017), 99-110.
[30] S. Singh, P. Chandra and J.B. Shukla, Modeling and analysis of the spread of carrier dependent infectious diseases with environmental effects, *J Biol Syst.*, **11**(3) (2003) 325-335.
[31] S. Singh, J.B. Shukla and P. Chandra, Modeling and analysis of the spread of malaria: environmental and ecological effects, *J Biol Syst.*, **13**(1) (2005), 1-11.
[32] S. Singh, J. Singh, J.B. Shukla, Modelling and analysis of the effects of density dependent contact rates on the spread of carrier dependent infectious diseases with environmental discharges, *Model Earth Syst Environ.*, **13**(5) (2019), 21-32.
[33] S. Singh, S. Chaudhry, M.S. Arora and R.K. Singh, Effects of temperature rise caused by greenhouse gases on the spread of food-borne diseases: a modeling study, *Jñānābha*, **54**(2) (2024), 328-342. DOI: `10.58250/jnanabha.2024.54233`
[34] S. Singh, S. Chaudhry, M.S. Arora, R.K. Singh and A.K. Misra, Modeling the effect of temperature rise due to atmospheric carbon dioxide on the outbreak of food-borne diseases, *J. Appl. Math. Comput.*, **71**(2) (2025), 2673-2701.
[35] S. Singh, Modeling the effect of global warming on the spread of carrier dependent infectious diseases, *Model Earth Syst Environ.*, **39**(3) (2017), 1-10.
[36] S. Singh and A. Omar, Modeling and analysis the effect of global warming on the Spread of carrier dependent infectious diseases, *Jñānābha*, **50**(1) (2020), 189-206.

[37] World Health Organization, Foodborne diseases, Geneva: *World Health Organization*, (2025). Available from: https://www.who.int/health-topics/foodborne-diseases#tab=tab_1

[38] WHO, *World Health Organization, Healh Topics, Food-borne diseases.* https://www.who.int/health-topics/foodborne-diseases#tab=tab_2

[39] World Meteorological Organization et al., *United in Science: High-level Synthesis Report of Latest Climate Science Information convened by the Science Advisory Group of the UN Climate Action Summit*, (2019). Available at: https://wedocs.unep.org/bitstream/handle/20.500.11822/30023/climsci.pdf.

[40] X. Wu, Y. Lu, S. Zhou, L. Chen and B. Xu, Impact of climate change on human infectious diseases: Empirical evidence and human adaptation, *Environ. Int.*, **86** (2016), 14–23. Available from: https://doi.org/10.1016/j.envint.2015.09.007